International Journal of Innovative Technology and Exploring Engineering (IJITEE)
ISSN: 2278-3075 (Online), Volume-3 Issue-6, November 2013

Optical and Magnetic Properties of Cu-Doped ZnO Nanoparticles

P. D. Sahare, Vipin Kumar

Abstract- Effect of Cu^{2+} ions doping on the photoluminescence (PL) and magnetic behavior of ZnO based host material nanoparticles have been investigated. A simple chemical route has been employed for the synthesis of Cu^{2+} incorporated ZnO nanoparticles for the present study. The prepared synergetic nanoparticles were analyzed for structural confirmation under X-ray diffraction (XRD) and Raman spectroscopic investigations. XRD patterns of the prepared nanoparticles of different Cu^{2+} concentrations reveal some shifting in the peak positions compared to that of the pure ZnO, which is attributed to the structural deformation in the presence of Cu^{2+} ions. Furthermore, transmission electron microscopy (TEM) studies have been performed for studying their morphology. TEM studies clearly show the formation of spherical and quasi spherical shaped nanoparticles of ~ 50 nm diameters. It is revealed from PL studies that the band-edge/UV emission decreases, whereas, the visible emission is found to increase with increase of the doping concentration. The decrease in the band-edge emission can be attributed to the substitution of Zn^{2+} by Cu^{2+} ions in the ZnO lattice. Beside, these optical properties, magnetic properties of ZnO nanoparticles has also been found to be affected by Cu doping, investigated using vibrating sample magnetometer (VSM). It has been observed from VSM study that the ferromagnetic behaviour of ZnO nanoparticles is found to enhance with increase in doping concentration.

Keywords- ZnO nanoparticles; Cu^{2+} doping; Photoluminescence; Magnetic properties; M-H loops; Surface defects.

I. INTRODUCTION

In last few decades, metal oxide nanoparticles were extensively investigated due to their gamut applications in the field of spintronics [1], photoelectronic [2], sensor [3], lasing devices [4] and light emitting diodes [5], etc. The properties of these nanomaterials incredibly altered due to quantum confinement and enhanced surface to volume ratio [6]. Among the most studied metal oxides nanoparticles, ZnO stands out due to its exceptional opto-electronical properties, low cost of synthesis, environmentally friendly and highly versatile device fabrication. It has a wide band gap (3.37 ev) and large excitonic binding energy of nearly 60 MeV [7].

In recent years, development of nanotechnology offers ZnO as one of the most promising dilute magnetic semiconductor (DMS) oxide material for futuristic spintronics devices, because of its curie temperature well above the room temperature. The physical and chemical properties of ZnO nanomaterials can be easily tailored as per the demand of device fabrication.

Various efforts have already been made to investigate the effect of doping elements (such as Ni, Co, Al, Li, Fe, Ce, Eu, etc.) on its electrical, optical and magnetic properties, essentially for practical industrial applications [8,9,10,11]. Many theoretical and experimental evidences suggested that ZnO doped with transition metals is a promising candidate for DMS. Although, origin of room temperature ferromagnetism of transition metals doped ZnO nanoparticles is still controversial, in both theory and experiments as well. Therefore, ZnO based DMS has attracted great attention for their possible particle application in the field of spintronic devices and the field is still open for further detailed discussions. In theory, there are two main explanations of origin of room temperature ferromagnetism in DMSs. First theory was proposed by Dietl et al. [12] which was based on carrier-mediated mechanism and according to his hole-mediated mechanism, it has been shown that p-type wide band gap DMSs possess high Curie temperature [13-20]. To induce sufficient ferromagnetic exchange interaction among the transition metal doped DMSs, a large density of mobile holes are required. Later on experimental observations at room temperature ferromagnetism of transition metal doped TiO_2 and ZnO provided a proof in the support of this theory partly [13,21,22]. But, in the case of n-type carriers or low concentration of mobile holes contradicts this theory [21, 23, 24]. After that Coey et al. employed another theory which was based on the bound magnetic polarons (BMP) model [20]. It was a spin-split band theory in which shallow donors controlled the magnetic moment of the dopants in n-type wide band gap DMSs. According to this theory, donor electrons in the impurity band get delocalized onto metal dopants to achieve sufficient donor dopant couplings which are further responsible for notable room temperature ferromagnetism. In other words, we can articulate the empty 3d states of transition metals to get hybridized with donor states at Fermi level. In case of DMSs, the kind of carriers, their mobility and density provide an opportunity to manipulate the ferromagnetic properties. Apart from the change in the magnetic properties due to transition metal doping, luminescence properties also get altered which are governed by defects states inside the ZnO matrix. Luminescence properties of ZnO are also of great interest due to their application in the field of lasing devices, light emitting diodes and optical sensing devices etc. ZnO has two emission bands one sharp band in UV region and another broad emission in visible region [25,26,27].

Manuscript published on 30 November 2013.
***Correspondence Author(s)**
Prof. P. D. Sahare, Department of Physics & Astrophysics, University of Delhi, Delhi, India.
Vipin Kumar, Department of Physics & Astrophysics, University of Delhi, Delhi, India.

The narrow UV emission band caused due to the radiative annihilation of excitons while the origin of the visible emission is still controversial. There are several reports already which demonstrate different proposition behind the visible emission of ZnO nanoparticles still there is no consensus on the origin of these emissions. A Large number of different hypotheses had been suggested in order to give more effective explanation [28,29,30,31]. For many years, it was assumed that the origin of the green luminescence was due to the oxygen vacancies or zinc interstitials [28,29]. Later, Djurisic et al.[30] proposed a new hypothesis that not only the oxygen vacancies or zinc interstitial are responsible for the visible emission, but there are certain surface defects available which could also affect the visible emission. While, Norberg and Gamelin found the presence of OH–groups attached to the surface and could act as sources for green emissions [31]. Photoluminescence properties of ZnO nanoparticles are very sensitive to the surface defects and size. Generally, in case of wet chemical synthesis some intermediate complexes or unreacted precursors remain attached to the surfaces of the nanoparticles and further act as a defect centres [32]. When transition metals are doped in ZnO host; they increase the defect density in the host and enhance the defect related emissions which put forward transition metals as suitable candidates for luminescence properties as well. Out of a variety of transition metals, copper is one of the most promising dopant because of its comparable size to Zn ion, which can easily substitute it.

In view of this, Cu doped ZnO nanoparticles have been synthesized for the evaluation of effect of doping concentration on the structural, magnetic and photoluminescence properties. The structural properties of the prepared Cu embedded ZnO nanoparticles were studies under X-ray diffraction studies. The change in the emission spectra with Cu doping concentration has been explained on the basis of the photoluminescence investigations in correlation with Raman study. Here, in the present investigation, we have also made an effort to explain the magnetic properties as well.

II. EXPERIMENTAL

A. Sample preparation

In the typical synthesis of ZnO nanoparticles, 0.1 M solution of zinc acetate and 0.1 M solution of charcoal activated carbon were prepared in propanol-2, separately. Then, both the solutions were mixed together and refluxed for few hours. After that, this solution was dried at ambient temperature. The grey powder thus obtained was further annealed at 700°C for 10 h to remove the carbon related contents and final product was designated as pristine ZnO (S_0).

Similar method has been used for the preparation of Cu doped ZnO nanoparticles except addition of $Cu(CH_3COO)_2.H_2O$ salt in the Zinc acetate solution under constant stirring. Different samples of ZnO nanoparticles with varying Cu concentrations, such as, 0.05, 0.10, 0.15 and 0.20 mol% were prepared and named as S_1, S_2, S_3, and S_4, respectively.

B. Characterization

X-ray powder diffraction (XRD) patterns of ZnO were recorded from 30 to 70°, using Cu K_α radiation (λ = 1.54056 Å) on "Bruker D8" X-ray diffractometer for structural analysis. Transmission electron microscopy (TEM) images and selected area electron diffraction (SAED) pattern were taken using Tecnai (300 kV), FEI, Holland. The PL studies on all the samples were carried out with Cary Eclipse Fluorescence Spectrophotometer (Varian make). Raman spectroscopic measurements have been performed on the prepared samples by Renishaw InVia Reflex Micro Raman spectrometer with air cooled argon laser of wavelength ~514.5 nm. Room temperature M-H loops are taken with maximum field ± 2.2 Tesla using Micro Scene EV9, USA.

III. RESULT AND DISCUSSION

A. Structural and Morphological study

Fig.1 shows the XRD patterns of all the samples (S_0–S_4). Intense diffraction peaks of the ZnO were observed at 31.34, 34.00, 35.84, 47.14, 56.24, 62.5, 66.00, 67.56 and 68.72 which were indexed to the (100), (002), (101), (102), (110), (103), (200), (112) and (201) planes, respectively, after comparing them with the data in the JCPDF file # 06-2151. It is evident from XRD patterns that all samples have Wurtzite structure (space group P^6_{3mc}) with lattice constants a = 3.256 Å and c = 5.212 Å. No obvious significant changes were observed in the XRD patterns of the Cu doped ZnO nanoparticles but the overall intensity of the XRD peaks decreased with increase in Cu concentration (as shown in Fig. 2), which indicates decrease in crystallinity of ZnO nanoparticles. However, careful observations indicated that the peak positions shift towards higher values. Especially, an intense peak located around 35.84° (101), when expanded, it was found that it does shift towards higher value with doping concentration increasing, which can be attributed to the substitution of Zn^{2+} by Cu^{2+} [33,34,35]. It is well reported in literature that the lattice parameters of the host materials gets altered in the presence of dopant material due to their

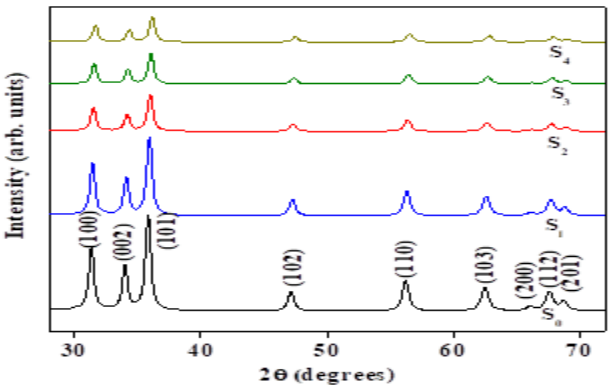

Fig. 1: XRD pattern of ZnO undoped and doped nanoparticles with different doping concentrations: S_0 (0.00 mol%), S_1 (0.05 mol%), S_2 (0.10 mol%), S_3 (0.15 mol%), and S_4 (0.20 mol%) different atomic radii and the dopant may situate in the voids or can replace Zn ions in the host lattice. Zn^{2+} ion can be easily replaced by Cu^{2+} ions because of their comparable ionic radii such as 0.096, 0.072 and 0.074 nm for Cu^+, Cu^{2+} and Zn^{2+}, respectively. Thus, the change in crystallinity and shift in peak positions of ZnO nanoparticles doped with Cu can also be attributed to shorter bonds of Cu-O and smaller size of [Cu-O_4] units as compared to Zn-O units [36].

Published By:
Blue Eyes Intelligence Engineering
and Sciences Publication (BEIESP)

However, the basic structure of ZnO nanoparticles remains the same (wurtzite type), which signifies that most of the Cu ions go in the lattice as substitutional ions replacing the Zn ions instead of getting in to void spaces.

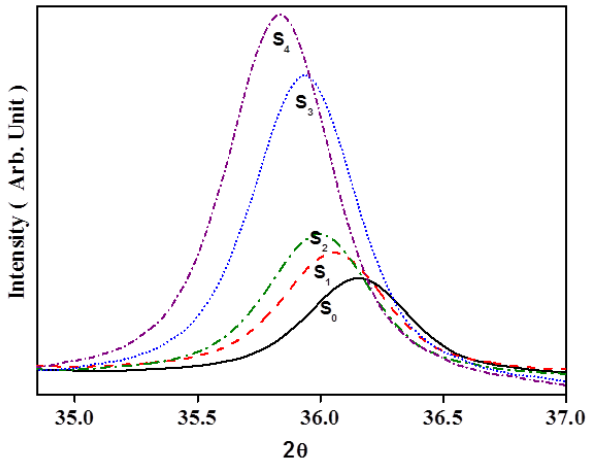

Fig. 2: Shifts in the (101) XRD peak of the sample doped with different concentrations of Cu^{2+}.

To further explore the effect the Cu doping on the structure of ZnO nanoparticles, lattice parameters of pure and doped samples (S_0–S_4) were calculated and are as tabulated in Table 1. It could be observed from Table 1 that the values of lattice parameters ('a' as well as 'c') decrease with doping concentration and is the resultant of different atomic radii of Cu ions and their positions in ZnO lattice [37,38]. To evaluate the effect of Cu ions doping on the crystallite size of ZnO nanoparticles, the average crystallite size of nanoparticles was calculated using the Scherrer's formula and found to be around 50, 48, 45, 44 and 41 nm for samples S_0, S_1, S_2, S_3 and S_4, respectively.

Sr. No.	Sample	a (Å)	c (Å)
1.	S_0 (Prinstine ZnO)	3.294	5.216
2.	S_1 (0.05 mol %)	3.281	5.216
3.	S_2 (0.10 mol %)	3.274	5.216
4.	S_3 (0.15 mol %)	3.269	5.211
5.	S_4 (0.20 mol %)	3.259	5.210

Table1: Lattice parameter values of undoped ZnO and Cu doped ZnO nanoparticles.

To get the information about the morphology and size of the ZnO nanoparticles, TEM studies had been carried out. TEM images of the undoped and Cu doped (0.05 mol %) ZnO nanoparticles are shown in figures 3(a) and 3(a′), respectively. It is observed from the TEM images that the size of ZnO nanoparticles decreases with Cu doping while shape the nanoparticles remain almost spherical type. Similar effect on the particle size of ZnO has already been reported with rare earth metal ion (Nd) doping [39,40]. The average particle size, calculated using TEM images by the Gaussian distribution (solid lines) of the corresponding histograms of undoped and Cu doped ZnO nanoparticles were 54 and 46 nm, respectively as shown in figures 3(b) and 3(b′), respectively. For closer investigations of the decrease in particles size with doping concentration, the magnified TEM images of undoped and Cu doped ZnO are also provided in figures 3(c) and 3(c′), respectively. The SAED pattern of undoped sample (fig. 3(d)) are indexed to the corresponding planes and well matched with the XRD pattern which indicates the long range ordering among the unit cells. The diffused rings in the SAED pattern (fig. 3(d′)) for Cu doped sample is attributed to the short range ordering among the unit cells caused by the doping which indicates the reduced crystallinity of Cu doped ZnO nanoparticles so results of SAED pattern also support the experimental evidences observed from the XRD results.

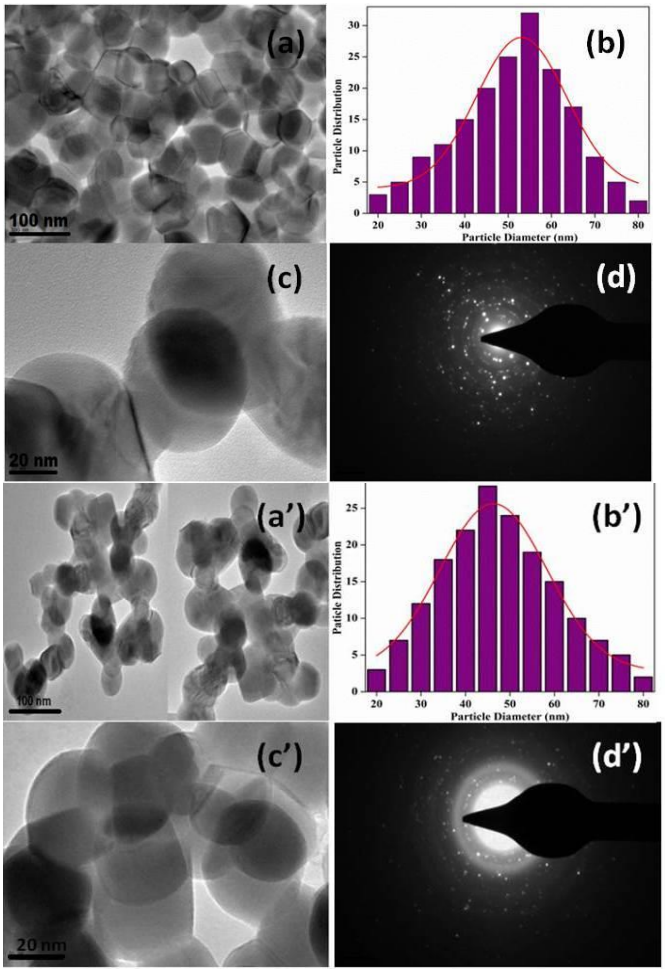

Fig. 3: TEM images of (a): undoped and (a′): 0.05 mol% Cu doped ZnO nanoparticles and their corresponding particle size distribution (b) and (b′). Figures (c) and (c′) show the TEM images at higher magnification and (d) and (d′) show the corresponding SEAD patterns.

B. Raman Analysis

ZnO with a space group C^4_{6v} has two formula units per primitive cell. ZnO has four atoms in each primitive cell. Each atom situated at C_{3v} sites leading to 12 phonon branches (9 optical and 3 acoustic). Optical phonon branches thus could be represented by an equation $\Gamma_{opt} = A_1 + 2B_1 + E_1 + 2E_2$ where A_1 and E_1 modes are polar, basically divided into two parts, transverse-optical (TO) and longitudinal-optical (LO) phonons, while the B_1 modes are Raman inactive [41].

Published By:
Blue Eyes Intelligence Engineering
and Sciences Publication (BEIESP)

The A_1 phonon vibrations are parallel to c-axis of the lattice so they are polarized parallel to the c-axis while E_1 phonon vibrations are perpendicular to the c-axis of the lattice so perpendicularly polarized to the c-axis. All modes correspond to a band with fixed wave number in the Raman spectrum whereas intensities of these bands totally depend on the scattering cross-section. E_2 modes are nonpolar and Raman active. These modes have two wave numbers classified as E_2^{low} and E_2^{high} mode. E_2^{low} associated with the motion of oxygen (O) atom and E_2^{high} with zinc (Zn) sublattice. Strong E_2^{high} mode is characteristic peak of the Wurtzite structure of ZnO lattice and is a measure of good crystallinity of the lattice. While E_1^{low} mode is due to the presence of oxygen vacancies and interstitial Zn ions. For the observation of A_1 (LO) phonon, c-axis of Wurtzite ZnO should be parallel to the sample surface. When perpendicular to the sample surface, E_1 (LO) phonon is found to be predominant [42].

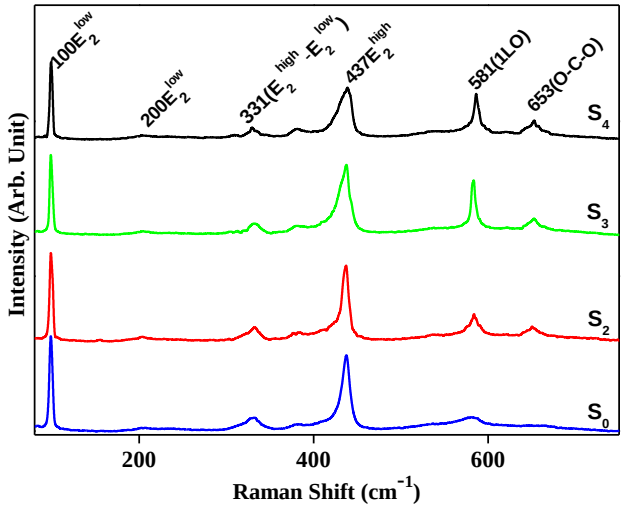

Figure 4: Raman spectra of doped (S_1, S_3, S_4) and undoped (S_0) samples.

Further molecular structure of ZnO nanoparticles has been further explored using Raman analysis and correlated with XRD and TEM results. Fig. 4 shows the Raman spectra of undoped and Cu doped ZnO samples with different concentration. The peaks at 100 cm^{-1} (E_2^{low}) and 437 cm^{-1} (E_2^{high}) are the nonpolar E_2 vibrational modes which are due to the vibration of Zn and O lattice in Wurtzite ZnO. The peak located at 200 cm^{-1} represents the $2E_2^{low}$ mode, whereas, the band located around 581 cm^{-1} is assigned to A_1 (LO) mode of ZnO nanoparticles [43,44,45,46]. Along with the characteristics peaks of ZnO, peak due to multiple-phonon scattering process and O-C-O symmetric bending were also observed, e.g., peak located at 335 cm^{-1} represents E_2^{high}-E_2^{low} mode (multi-phonon scattering) while the peak at 653 cm^{-1} corresponds to the O-C-O symmetric bending. The presence of highly intense E_2^{low} and E_2^{high} bands indicates the highly crystalline nature of Wurtzite ZnO nanostructure. The intensity of these bands found to decrease with increase in Cu concentration, which can be attributed to the lattice distortion in the ZnO matrix via doping as also observed from XRD studies. Furthermore, it has been observed that the band located around 437 cm^{-1} (E_2^{high}) becomes more and more broader with doping concentration along with minor shifting and enhanced asymmetry towards lower wavenumber side. The FWHM value of E_2^{high} mode is found to be 8.57, 10.67, 14.27 and 17.51 cm^{-1} for samples S_1, S_2, S_3 and S_4, respectively. The decrease in the intensity of E_2^{high} peak with Cu concentration in the ZnO matrix confirms variation in defects states of ZnO [47]. For more visualization of resultant changes, Lorentzian curve fitting results of the 1LO (581 cm^{-1}) mode of ZnO nanoparticles are shown in Fig. 5. For all forms of ZnO like bulk, thin-films and nanoparticles of ZnO, this broad asymmetric peak (581 cm^{-1}) associated with 1LO mode and the intensity increases with the increase in Cu concentration [48,49,50]. This band is deconvoluted into two components positioned at 539 and 581 cm^{-1} (spectra for S_0) and assigned to A_1 (LO) and E_1 (LO) modes, respectively [48]. The A_1 (LO) mode shifts towards the higher wave number side from 539, 543, 551 and 558 cm^{-1} with the increase in the concentration, while, there is only a minor shifting in the peaks position of E_1 (LO) mode from 581, 581, 582 and 583 cm^{-1} for samples S_1, S_2, S_3 and S_4, respectively.

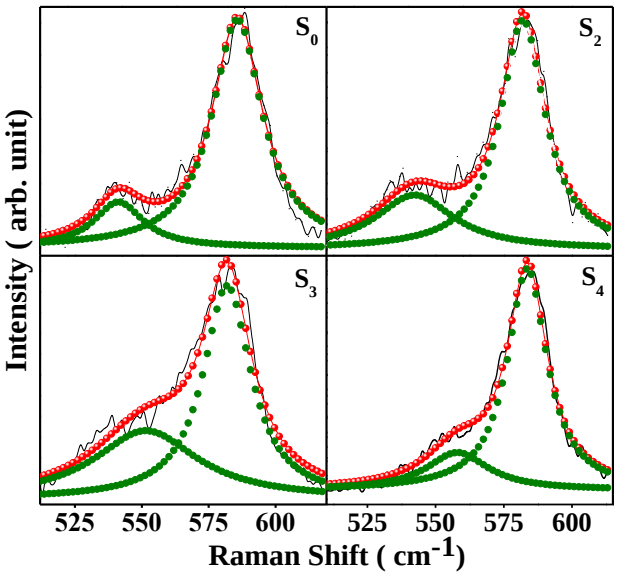

Figure 5: Deconvolution 1LO mode into two peaks for undoped (S_0) and doped (S_1, S_3, S_4) samples.

The presence of these two modes, i.e., E_1 (LO) and A_1 (LO) in the Raman spectra, confirms the random orientation of ZnO [48], which is further supported by the decrease in the separation between A_1 (LO) and E_1 (LO) mode with increase in the Cu concentration. However, no extra band was observed associated with CuO, Cu_2O or complexes of metals like Cu-Zn, but only the Raman spectra of ZnO gets altered.

C. Photoluminescence

To reveal the effect of Cu^{2+} doping on the photoluminescence properties of the ZnO nanoparticles, PL measurement had been carried out at room temperature. Figure 6 shows PL spectra of the undoped and Cu^{2+} doped ZnO nanoparticles. ZnO nanoparticles are well-known for its emission bands and generally, two major bands are observed in the PL emission spectrum of ZnO associated with visible emission around at ~543 (2.28 eV) nm and near band-edge emission located at ~384 nm (3.32 eV). The slight shifting in band edge peak confirms the existence of doping states of ZnO.

Published By:
Blue Eyes Intelligence Engineering and Sciences Publication (BEIESP)

Similar types of effects had already reported with RE (Nd, Er and Ce) doped ZnO [51]-[53]. The broad emission band (543 nm) is considered to be the superposition of green and yellow-orange emission bands. There are several reports available which reveals that the oxygen vacancies responsible for the green emission are mainly located at the surface [54] whereas, the presence of OH groups or deep level defects are responsible for yellow emission band [12], [55]. The surface of ZnO nanoparticles consists of some positive charge states (surface defects) due presence of oxygen ion vacancies at the surface, as a result surface has a tendency to get some residual intermediate compounds

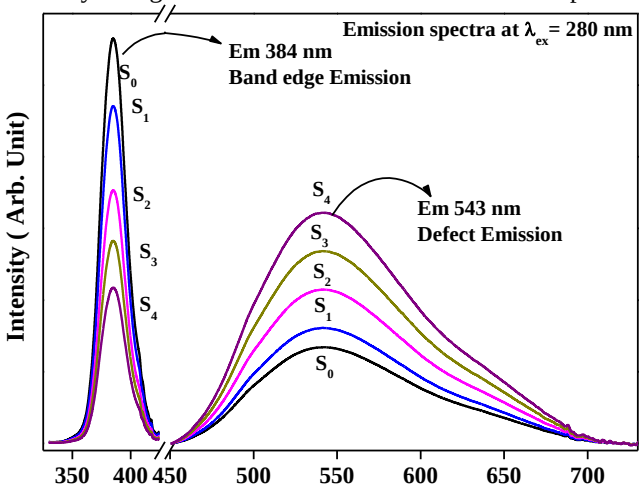

attached on the surface in the form of an acetate or OH groups which further acts as defect centres and affect the green emissions [56].

Figure 6: Emission spectra of Cu^{2+} doped and undoped samples at excitation wavelength 284 nm.

This is more so in the present case as the material is prepared through the aqueous solution and using acetate salts of the ingredients. These residuals groups are roughly bound on the surface by means of dangling bonds [57]. It is difficult of distinguish between the emission spectra due to surface defect and impurities added in the host due to overlapping of these bands in the visible region. To overcome from this problem, the visible broad emission band had been deconvoluted into two components (located at ~543 and 615 nm). Fig. 7(a and b) show the deconvoluted spectra of undoped and Cu^{2+} doped ZnO nanoparticles. Peak located at 543 nm (2.28 eV) could be attributed to the O_i (oxygen interstitial) and V_0 (oxygen vacancies), while the peak at 615 nm (2.02 eV) is due to OH group [55,58,63]. The intensity of the deconvoluted peak (543 nm), due to oxygen interstitials and oxygen vacancies, (i.e., 2.28 eV), increases with an increase in doping concentration which further confirms the increase in the surface defect states on doping level increasing in ZnO nanoparticles. Since, the nanoparticles posses enhanced surface to volume ratio, which provides additional sites for surface residues, such as, OH^- groups. This can be depicted from the deconvoluted component associated with the OH group, whose intensity increases with increase in Cu concentration. Since, the particle size of ZnO nanoparticles decrease with Cu doping which leads to further enhancement in surface to volume ratio and hence, enhanced surface defect (number of OH^- groups attached) or increase in the concentration of oxygen vacancies [64]. This causes in enhancement in PL intensity of the band located at 615 nm associated with surface defect (oxygen vacancies) states of ZnO nanoparticles. Moreover, Cu^{2+} only replaces Zn^{2+} ions without altering the oxygen concentration. Thus, the change in the concentration of oxygen ion vacancies is not the result of replacement of Zn^{2+} ions by Cu^{2+} but, it is because of the change in the surface to volume ratio due to decrease in

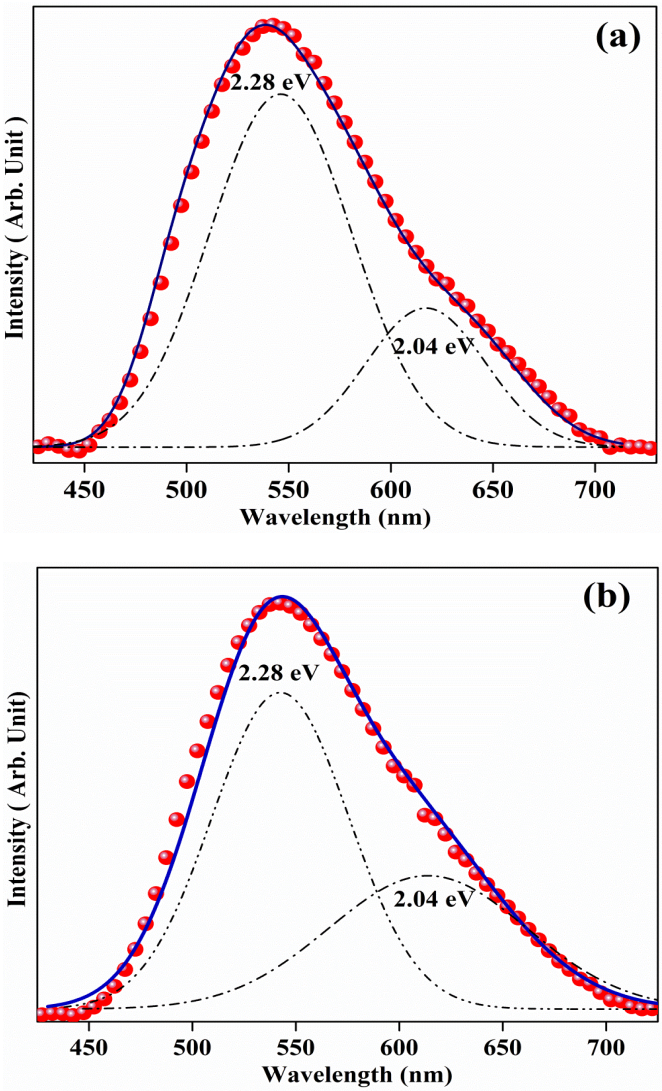

particle size [65,66]. Therefore, the PL study reveals that doping of Cu^{2+} ions in the ZnO host leads to the increase in the concentration of surface defects and makes it a suitable

Figure 7: a) Deconvolution of visible emission peak of undoped sample (S_0), b) Deconvolution of visible emission peak of doped sample (S_4).

candidate for the potential application in solid state lighting or other optoelectronic applications. Increased peak intensity of visible emission with the Cu^{2+} concentration can be directed to the enhancement in the defect states inside the ZnO nanoparticles. The results obtained from PL study are well matched with reports in the literature show that the PL emission intensity (band-edge UV as well as visible band due to defect states) could be articulated by proper doping. The study is important for understanding the defect states and their effects on optical properties.

Published By:
Blue Eyes Intelligence Engineering
and Sciences Publication (BEIESP)

E. Magnetic measurements

The effect of Cu doping on the magnetic properties of ZnO nanoparticles has also been studied by VSM measurements performed at room temperature. The presence of defect states of ZnO are responsible for magnetic properties of ZnO [12,20,24] and such behaviour of ZnO is further explored with Cu doping with different concentration. Figure 8 shows the magnetization versus magnetic field (M-H) hysteresis loops for ZnO:Cu^{2+} nanoparticles. All plots of the magnetization hysteresis reveal ferromagnetic behaviour of ZnO nanoparticles with enhanced magnetic properties with Cu doping in ZnO matrix. The saturation magnetization was found to be 0.011, 0.021, 0.026, 0.043 and 0.063 emu/gm along with improved coercivity 18, 40, 93, 158 and 181 Oe for the samples S_0, S_1, S_2, S_3 and S_4, respectively. There are several reports available which has already shown that magnetic properties of transition metal doped ZnO nanoparticles are mediated by the ferromagnetic exchange between the dopant ion and defects states available in the ZnO [12, 20, 24, 27, 28, 29, 67].

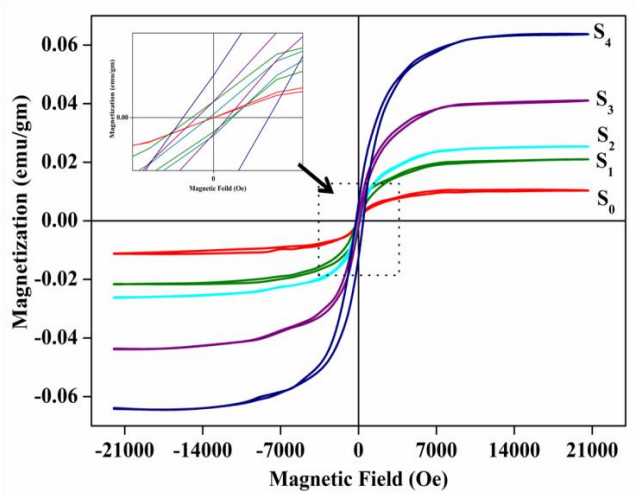

Figure 8: Room temperature hysteresis measurement for doped and undoped samples while inset shows the magnified view of hysteresis loop near the mid-point.

Since, the Cu^{2+} ions doped samples have larger oxygen vacancies which are responsible for long-range ferromagnetism order and hence, enhanced magnetic properties. The improved coercivity with Cu^{2+} concentration is as shown in the inset of Fig. 8. Such type of magnetic behaviour can be understood on the basis of bound magnetic polarons (BMP) model suggest by Coey *et al.* [20, 24]. This model suggested a spin-spilt impurity band theory in which shallow defect (donors) control the dopant magnetic moment alignment in the wide band gap DMSs. Bound electrons in defects like oxygen vacancies can induce a ferromagnetic coupling with Cu^{2+} ions through an indirect exchange. These donor electrons in the impurity bands overlaps onto dopant Cu^{2+}, which is further responsible for the remarkable increase in the donor-dopant ferromagnetic coupling. In the present study, we have also observed enhanced defect states with the concentration of Cu^{2+}, which can provide more ferromagnetic coupling. Moreover, the empty 3d states of Cu^{2+} ions hybridizes with the donor electron states at the Fermi level which set up a platform to manipulate the ferromagnetic characteristics of ZnO nanoparticles as well and give rise to long-range ferromagnetic order in the sample. Similar kind of results have been reported earlier with Mn, Co and Ni-doped ZnO [27-29] and support the results of increase in the defects states with Cu^{2+} doping, which leads to enhance PL and magnetic properties of ZnO nanoparticles in the present case.

IV. CONCLUSIONS

In summary, ZnO nanoparticles were successfully synthesized by simple chemical route. TEM studies confirm the growth of ZnO nanoparticles with some agglomeration. It has also been found that the average particles size of the prepared ZnO nanoparticles decreases with Cu doping. For as prepared sample, the average particle size (as seen in TEM images) was 54 nm while the same for the Cu doped sample (S_4) was 46 nm. Particle size calculated from XRD and TEM shows good agreement. XRD and Raman results demonstrated that Cu ions successfully substitute Zn ions in the Wurtzite hexagonal structure of ZnO nanoparticles. PL intensity of near band-edge/UV band emission is found to decrease due to such substitutions, whereas, appreciable increase in green emission was observed with increase in the concentration of Cu ions. Room temperature VSM study demonstrates that the saturation magnetization and coercivity of samples increases with Cu doping. Finally, it could be concluded that defects play an important role in manipulating the ferromagnetic as well as photoluminescence properties of ZnO nanoparticles.

V. ACKNOWLEDGMENT

Authors would like to thank the University of Delhi for providing CIF (Central Instrumentation Facility at University Scientific Instrumentation Centre) and partial funding under the R&D Scheme.

REFERENCES

1. T. Meron, G. Markovich, *J. Phys. Chem. B.* 109, 20232 (2005).
2. S. Liang, H. Sheng, Y. Liu, Z. Huo, Y. Lu, H. Shen, *J. Cryst. Growth*, 225, 110 (2001)
3. S.T. Shishiyanu, T.S. Shishiyanu, O.I. Lupan, *Sens. Actuators B*, 107, 379 (2005)
4. M.H. Huang, S.Mao, H. Feick, H. Yan, Y.Wu, H. Kind, E.Weber, R. Russo P. Yang, *Science*, 292, 1897 (2001)
5. N. Saito, H. Haneda, T. Sekiguchi, N. Ohashi, I. Sakaguchi, K. Koumoto, *Adv. Mater.*, 14, 418 (2002)
6. Yi Ma, C. Ricciuti, T. Miller, J. Kadlowec and H. Pearlman, *Energy & Fuels*, 22 3695 (2008)
7. R. Chen, B. Ling, X. W. Sun, H. D. Sun, *Adv. Mater*, 23, 2199 (2011)
8. F. Li, Y. Yuan, J. Luo, Q. Qin, J. Wu, Z. Li, X. Huang, *Applied Surface Science*, 256, 6076 (2010)
9. Q. Wang, B. Geng, S. Wang, *Environ. Sci. Technol.* 43, 8968 (2009)
10. M. Ungureanu, H. Schmidt, H. V. Wenckstern, H. Hochmuth, M. Lorenz, M. Grundmann, M. Fecioru-Morariu, G. Guntherodt, *Thin Solid Films*, 515, 8761(2007)
11. Y. Zhou, S. X. Lu, W. G. Xu, *Environmental Progress & Sustainable Energy*, 28, 226 (2009)
12. T, Dietl, H. Ohno, F. Matsukura, J. Cibert and D. Ferrand, *Science*, 287 1019 (2000)
13. K. Sato, H. Katayama-Yoshida, *Semi. Sci. Technol*, 17, 367 (2002)
14. Y. Matsumoto, M. Murakami, T. Shono, T. Hasegawa, T. Fukumura, M. Kawasaki, P. Ahmet, T. Chikyow, S. Koshihara and H. Koinuma, *Science*, 291, 854 (2001)
15. S. J. Pearton, D. P. Norton, K. Ip, Y. W. Heo and T. Steiner, *J. Vac. Sci. Technol. B* 22, 932 (2004)
16. K. R. Kittilstved, N. S. Norberg and D. R. Gamelin, Phys. Rev. Lett, 94, 147209 (2005)

Published By:
Blue Eyes Intelligence Engineering and Sciences Publication (BEIESP)

17. G. Clavel, M. G. Willinger, D. Zitoun and N. Pinna, *Adv. Funct. Mater.* 17, 3159 (2007)
18. T. Dietl, H. Ohno and F. Matsukura, *Phys. Rev. B*, 63 195205 (2001)
19. A. Kaminski, S. Das Sarma, *Phys. Rev. Lett*, 88, 247202 (2002)
20. J. M. D. Coey, M. Venkatesan and C. B. Fitzgerald, *Nat. Mater*. 4, 173 (2005)
21. K. Ueda, H. Tabata and T. Kawai, *Appl. Phys. Lett.* 79, 988 (2001)
22. S. W. Lim, M. C. Jeong, M. H. Ham, J. M. Myoung, *J. Appl. Phys.* 43, 280 (2004)
23. H. Saeki, H. Tabata, T. Kawai, *Solid State Commun.* 120, 439 (2001)
24. J. M. D. Coey, M. Venkatesan, C. B. Fitzgerald, *Nature Mater*. 4 173 (2005)
25. A. V. Dijken, E. A. Meulenkamp, D. Vanmaekelbergh, A. Meijerink, *J. Lumin.*, 87, 454 (2010)
26. I. Shalish, H. Temkin, V. Narayananmurti, *Phys. Rev. B*, 69, 245401 (2004)
27. Y. M. Sun, Ph.D. thesis, University of Science and Technology of China (2000)
28. U. Koch, A. Fojtik, H. Henglein, *Chem. Phys. Lett.* 122, 507 (1985)
29. L. Spanhel, M. A. Anderson, *J. Am. Chem. Soc.* 113, 2826 (1991)
30. A. B. Djurisic, W. C. H. Choy, Y. A. L. Roy, Y. H. Leung, C. Y. Kwong, K. W. Cheah, T. K. Gundu Rao, W. K. Chan, H. F. Lui, C. Surya, *Adv. Funct. Mater.* 14, 856 (2004)
31. N. S. Noberg, D. R. Gamelin, *J. Phys. Chem. B*, 109, 20810 (2005)
32. S. Sakohara, M. Ishida, M. A. Anderson, *J. Phys. Chem. B*, 102, 10169 (1998)
33. T.S. Herng, S.P. Lau, S.F. Yu, H.Y. Yang, L. Wang, M. Tanemura, J.S. Chen, *Appl. Phys. Lett.*, 90, 032509 (2007).
34. Z. Zhang, J. B. Yi, J. Ding, L. M. Wong, H. L. Seng, S. J. Wang, J. G. Tao, G. P. Li, G. Z. Xing, T. C. Sum, C. H. Alfred Huan, T. Wu, *J. Phys. Chem. C*, 112, 9579 (2008).
35. O. Lupan, Th. Pauporté, T. Le Bahers, B. Viana, I.Ciofini, *Advanced Functional Materials*, 21 3564 (2011).
36. Q. Ma, D.B. Buchholz, R.P.H. Chang, *Physical Rev.B*, 78, 214429 (2008).
37. O. Lupan, T. Pauporté, L. Chow, B. Viana, F. Pellé, B. Roldan Cuenya, L.K. Ono, H. Heinrich, *Appl. Surf. Science*, 256 1895 (2010)
38. O. Lupan, T. Pauporté, B. Viana, P. Aschehoug, *Electrochimica Acta*, 56, 10543 (2011)
39. Z. Y. Huang, P. Luo, M. Chen, S.R. Pan, D.H. Chen, *Materials Letters*, 65, 2345 (2011)
40. Y. Zhou, S. X. Lu, W. G. Xu, *Environmental Progress & Sustainable Energy*, 28, 226 (2009)
41. T. C. Damen, S.P.S. Porto, B. Tell, *Phys. Rev.* 142, 570 (1966)
42. N. Ashkenov, G. Wagner, H. Neumann, B.N. Mbenkum, C. Bundesmann, V. Riede, *J. Appl. Phys.* 93 126 (2003)
43. J. Xing, Z. H. Xi, Z. Q. Xue, X. D. Zhang, J. H. Song, R. M. Wang, *Appl. Phys. Lett.*, 83, 1689 (2003)
44. S.H. Jeong, J.K. Kim, B.T. Lee, *J. Phys. D: Appl. Phys*, 36, 2017 (2003)
45. M. Scepanovic, M. Grujic-Brojcin, K. Vojisavljevic, S. Bernik, T. Sreckovic, *J. Raman Spectrosc*, 41, 914 (2010)
46. R. D. Yang, S. Tripathy, Y. Li, H. J. Sue, *Chem. Phy. Lett.*, 411, 150 (2005)
47. M. S. Cepanovic, M. Grujic-Brojcin, K. Vojisavljevic, S. Bernik, T. Sreckovic, *Journal of Raman Spectroscopy*, 41, 914 (2010)
48. B. Cao, W. Cai, H. Zeng, G. Duan, *Journal of Applied Physics*, 99, 073516 (2006)
49. T.C. Damen, S.P.S. Porto, B. Tell, *Physical Review*, 142, 570 (1966)
50. B. Yang, A. Kumar, P. Feng, R. S. Katiyar, *Applied Physics Letters*, 92, 233112 (2008).
51. M. Subramanian, P. Thakur, S. Gautam, K.H. Chae, M. Tanemura, T. Hihara, *J. Phys. D: Appl. Phys.* 42 105410 (2009)
52. M. H. Choi, T. Y. Ma, *Mater. Lett.* 62 , 1835 (2008)
53. Z. Sofiani, B. Derkowska, P. Dalasiński, M. Wojdyła, S. Dabos-Seignon, M. A. Lamrani, *Opt. Commun.* 267, 433 (2006)
54. D. Li, Y. H. Leung, A. B. Djurisic, Z. T. Liu, M. H. Xei, S. L. Shi, S. J. Xu, W. K. Chan, *Appl. Phys. Lett.* 85, 1601 (2004)
55. K. H. Tam, C. K. O. Cheung, Y. H. Leung, A. B. Djurisic, C. C. Ling, C. D. Beling, S. Fung, W. M. Kwok, W. K. Chan, D. L. Phillips, L. Ding, W. K. Ge, *J. Phys. Chem. B* 110, 20865 (2006)
56. S. Sakohara, M. Ishida, M. A. Anderson, *J. Phys. Chem. B*, 102, 10169 (1998).
57. R. M. Raghvendra, S. Yadav, A. C. Pandey, S. S. Sanjay, C. Dar, *Journal of Luminescence*, 130, 365 (2010).
58. B. Lin, Z. Fu, *Appl. Phys. Lett.*, 79, 943 (2001).
59. K. Vanheusden, C. H. Seager, W. L. Warren, D. R. Tallant and J. A. Voigt, *Appl. Phys. Lett.* 68, 15 (1996).
60. H. Zhou, H. Alves, D. M. Hofmann, W. Kriegseis, B. K. Meyer, G. Kaczmarczyk, A. Hoffmann, *Appl. Phys. Lett.* 80, 210 (2002).
61. A.F. Kohan, G. Ceder, D. Morgan, *Phys. Rev. B* 61, 22 (2000)
62. L. S. Vlasenko, *Physica B*, 404, 4774 (2009)
63. J. Qiu, X. Li, F. Zhuge, X. Gan, X. Gao, W. He, S. J. Park, H. K. Kim, Y. H. Hwang, *Nanotechnology*, 21, 195602 (2010)
64. H. M. Xiong, D. G. Shchukin, H. Mohwald, Y. Xu, Y. Y. Xia, *Angew. Chem. Int. Ed*., 48, 2727 (2009)
65. M. Haase, H. Weller, A. Henglein, *J. Phys. Chem.* 92, 482 (1988)
66. J. Antony, S. Pendyala, D.E. McCready, M.H. Engelhard, D. Meyer, A. Sharma, Y. Qiang, *IEEE Trans. Magn.* 42, 2697 (2006)
67. S. Mala, J. Narayana, S. Nori, J. T. Prater, D. Kumar, *Solid Stat. Comm*. 150, 1660 (2010).

AUTHOR PROFILE

Prof. P. D. Sahare is presently working as Professor of Physics in the Department of Physics & Astrophysics, University of Delhi, India. He is also the Radiation Safety Officer (RSO) at the institution.

He graduated from RTM Nagpur University, Nagpur, India. He did his Master's degree in Physics in 1985. He started his research career and acquired M. Phil. in 1987 and Ph. D. in the field of luminescence in 1990 from the same institution. He also worked as a faculty in his parent department before he was invited as a Visiting Scientist in the Department of Polymer Science & Engineering, University of Massachusetts, Amherst, USA.

He joined the University of Delhi in 1993 as Assistant Professor. He also worked as Professor of Physics at the University of Pune during 2006-08. His fields of interest are: Luminescence and its applications, Development of Luminescent phosphors, Laser materials, sensors and detectors, interaction of nanomaterials for biotechnological applications. His other interests are different detection techniques, especially, Radiation dosimetry, Medical and Environmental dosimetry, etc.

His recent work on TLD nanophosphors is well appreciated and cited. He also has worked on ZnS, ZnO and mixed nanocrystalline systems for their applications as effective photo-catalysts, detectors and optoelectronic materials. He has successfully completed some research projects funded by DST, ISRO, IUAC and DRDO.

He has collaborations with CSIR, DRDO labs, Inter University Accelerator Centre, New Delhi and also with several other institutions and universities. He also has active collaboration with P. N. Lebedev Physical Institute, Moscow, Russia and Kyung Hee University Seoul, South Korea. He has organized several National and International conferences. Till date several students have successfully completed their M. Tech. internship projects. Also 10 M. Phil. and 10 Ph. D. students have successfully completed their research work under his supervision.

He is Life Member of Luminescence Society of India and President, Luminescence Society of India (Delhi Chapter). He is Editor-in-Chief of Luminescence and Applications, Columbia International Publishing, USA and on Editorial Boards of several international journals.

Vipin Kumar had received his M.Sc. degree in Physics with specialization in advanced solid state physics (experimental) from Department of Physics & Astrophysics, University of Delhi, Delhi, India. He is currently working as a Ph. D. Student in the field of semiconducting nanomaterials and their applications.

Published By:
Blue Eyes Intelligence Engineering and Sciences Publication (BEIESP)